Diabetologia (2012) 55:1114–1127
DOI 10.1007/s00125-012-2456-x

ARTICLE

The proteomic signature of insulin-resistant human skeletal muscle reveals increased glycolytic and decreased mitochondrial enzymes

J. Giebelstein · G. Poschmann · K. Højlund · W. Schechinger · J. W. Dietrich · K. Levin · H. Beck-Nielsen · K. Podwojski · K. Stühler · H. E. Meyer · H. H. Klein

Received: 8 October 2011 / Accepted: 19 December 2011 / Published online: 27 January 2012

Abstract
Aims/hypothesis The molecular mechanisms underlying insulin resistance in skeletal muscle are incompletely understood. Here, we aimed to obtain a global picture of changes in protein abundance in skeletal muscle in obesity and type 2 diabetes, and those associated with whole-body measures of insulin action.
Methods Skeletal muscle biopsies were obtained from ten healthy lean (LE), 11 obese non-diabetic (OB), and ten obese type 2 diabetic participants before and after hyperinsulinaemic–euglycaemic clamps. Quantitative proteome analysis was performed by two-dimensional differential-gel electrophoresis and tandem-mass-spectrometry-based protein identification.
Results Forty-four protein spots displayed significant ($p<0.05$) changes in abundance by at least a factor of 1.5 between groups. Several proteins were identified in multiple spots, suggesting post-translational modifications. Multiple spots containing glycolytic and fast-muscle proteins showed increased abundance, whereas spots with mitochondrial and slow-muscle proteins were downregulated in the OB and obese type 2 diabetic groups compared with the LE group. No differences in basal levels of myosin heavy chains were observed. The abundance of multiple spots representing glycolytic and fast-muscle proteins correlated negatively with insulin action on glucose disposal, glucose oxidation and lipid oxidation, while several spots with proteins

J. Giebelstein, G. Poschmann and K. Højlund contributed equally to this work.

Electronic supplementary material The online version of this article (doi:10.1007/s00125-012-2456-x) contains peer-reviewed but unedited supplementary material, which is available to authorised users.

J. Giebelstein · W. Schechinger · J. W. Dietrich · H. H. Klein (✉)
Medizinische Klinik I, Berufsgenossenschaftliches Universitätsklinikum Bergmannsheil,
Klinikum der Ruhr Universität Bochum,
Bürkle-de-la-Camp-Platz 1,
44789 Bochum, Germany
e-mail: harald.klein@rub.de

G. Poschmann · K. Podwojski · K. Stühler · H. E. Meyer
Medizinisches Proteom-Center, Ruhr Universität Bochum,
Bochum, Germany

K. Højlund · K. Levin · H. Beck-Nielsen
Diabetes Research Center, Department of Endocrinology,
Odense University Hospital,
Odense, Denmark

W. Schechinger
Bioavid Diagnostics,
Dieburg, Germany

K. Podwojski
Department of Statistical Methods in Genetics and Chemometrics,
Technical University Dortmund,
Dortmund, Germany

K. Stühler
Molecular Proteomics Laboratory,
Heinrich Heine Universität Düsseldorf,
Düsseldorf, Germany

involved in oxidative metabolism and mitochondrial function correlated positively with these whole-body measures of insulin action.
Conclusions/interpretation Our data suggest that increased glycolytic and decreased mitochondrial protein abundance together with a shift in muscle properties towards a fast-twitch pattern in the absence of marked changes in fibre-type distribution contribute to insulin resistance in obesity with and without type 2 diabetes. The roles of several differentially expressed or post-translationally modified proteins remain to be elucidated.

Keywords Glycolysis · Insulin resistance · Mitochondria · Obesity · Proteome analysis · Skeletal muscle · Type 2 diabetes mellitus

Abbreviations

2D-DIGE	Two-dimensional differential gel electrophoresis
ACO2	Aconitate hydratase
ACTA1	Actin, α skeletal muscle
ATP5A1	ATP synthase subunit-α
ATP5B	ATP synthase subunit-β
ENO3	β-Enolase
ESI	Electrospray ionisation
GAPDH	Glyceraldehyde-3-phosphate dehydrogenase
GBAS	NipSnap-homologue-2
GDR	Glucose disposal rates
HES1	ES1 protein homologue
LE	Healthy lean
MYH	Myosin heavy chain
MYL	Myosin light chain
MYLPF	Myosin regulatory light chain 2, skeletal muscle
NOGM	Non-oxidative glucose metabolism
OB	Obese non-diabetic
PGAM2	Phosphoglycerate mutase-2
PKM2	Pyruvate kinase
PTM	Post-translational modification
PYGM	Glycogen phosphorylase, muscle form
TCA	Tricarboxylic acid
TNNT3	Fast skeletal muscle troponin-T

Introduction

Insulin resistance of skeletal muscle is a major metabolic feature in obesity and a key factor in the pathogenesis of type 2 diabetes [1]. The underlying molecular mechanisms are complex and still incompletely understood. Insulin signalling is impaired at several levels [1, 2], but whether these changes are primary or secondary to the metabolic changes remains unclear [2]. Inflammation and cytokine signalling appear to be important, and recent studies have linked insulin resistance with mitochondrial dysfunction. This includes reduced mitochondrial content and in some [2–5], but not all, studies, reduced mitochondrial functional capacity [2, 4, 6–12].

While hypothesis-driven investigations have elucidated important details of the complex mechanism leading to insulin resistance, hypothesis-free global approaches such as microarray-based transcriptional profiling or quantitative proteome analysis have the advantage of investigating the whole complexity. Thus, evidence for patterns of changes can be provided and, potentially, new hypotheses generated. The transcriptomic and proteomic approaches are complementary as changes in mRNA levels do not necessarily mirror changes in the abundance of the proteins encoded by these genes, and potentially important post-translational modifications (PTMs) can only be detected by proteomics.

There have been several previous approaches to the study of the human skeletal muscle proteome [13, 14] and its alterations in insulin-resistant muscle [15–18]. Two studies have used the two-dimensional gel approach [15, 16]. Although these investigators described several differences in protein abundance between insulin-sensitive and -insensitive muscle, their studies were somewhat limited by the proteomic technologies available at that time. Thus, lower resolution of the spots, lower sensitivity and/or lower dynamic range of the staining methods and protein identification by matrix-assisted laser desorption/ionisation (MALDI)-time of flight (TOF) MS rather than high-sensitivity HPLC-electrospray ionisation (ESI)-MS/MS (tandem mass spectrometry) made it difficult to detect and identify changes in protein abundance. Moreover, these earlier attempts involved study groups that were less well matched or rather small. Another more recent study investigated muscle from healthy lean, obese non-diabetic and obese type 2 diabetic individuals using one-dimensional gel separation with SDS-PAGE followed by HPLC-ESI-MS/MS-based identification and quantification [17], and reported significant changes in the abundance of 15 proteins.

Within the last years, the combination of two-dimensional differential gel electrophoresis (2D-DIGE) and fluorescence staining of proteins followed by protein identification using high-sensitivity MS/MS methods has proven to be a suitable gel-based method for the quantification of changes in abundance of proteins or patterns of proteins in human tissues and has recently been used to compare the human skeletal muscle mitochondrial proteome before and after endurance exercise training [14]. Here, we applied this technology to investigate alterations of the skeletal muscle proteome in obesity and type-2-diabetes-associated insulin resistance, respectively. Muscle biopsies obtained from healthy lean (LE), obese non-diabetic (OB), and matched obese type 2-diabetic individuals before and after hyperinsulinaemic–euglycaemic clamps were

individually analysed. In addition to the comparison of the three participant groups, associations of spot volumes with rates of glucose disposal (GDR) and other variables were explored.

Methods

Participants Ten LE and 11 OB individuals with normal glucose tolerance and no family history of diabetes, and ten obese individuals with type 2 diabetes were included in the study (Table 1). In the obese type 2 diabetes group, diabetes had been diagnosed for 2.8±0.9 years and was treated by diet alone, sulfonylurea, metformin or human insulin (four, five, one and three participants, respectively). Metformin, sulfonylurea or NPH insulin were withdrawn 1 week before the study, fast-acting human insulin was withdrawn after the last meal the evening before. Patients were GAD-65-antibody negative and without signs of diabetic retinopathy, nephropathy, neuropathy and macrovascular complications. Informed consent was obtained before participation, and the study was approved by the local ethics committee and performed in accordance with the Helsinki declaration.

Clamp experiments and biopsy procedures These were performed as described [19]. Briefly, after an overnight fast the participants underwent hyperinsulinaemic–euglycaemic clamps (40 mU m^{-2} min^{-1} insulin for 4 h) combined with whole-body indirect calorimetry; GDR, glucose oxidation, lipid oxidation and non-oxidative glucose metabolism (NOGM) were assessed as described [19, 20]. In the obese type 2 diabetes group, plasma glucose was allowed to decline to 5.5 mmol/l before glucose infusion was initiated. Muscle biopsies were obtained from the vastus lateralis muscle before and after the insulin infusion, and were frozen in liquid nitrogen [19].

Table 1 Characteristics of individuals in the LE, OB and obese type 2 diabetes groups

Characteristic	LE	OB	T2D
n (male/female)	10 (5/5)	11 (6/5)	10 (6/4)
Age (years)	51±1	49±1	50±1
BMI (kg/m^2)	24.2±0.5	33.7±1.4*	33.5±1.1*
HbA_{1c} (%)	5.5±0.1	5.4±0.1	7.8±0.5*†
HbA_{1c} (mmol/mol)	37±0.8	36±1.0	61±5.9*†
Fasting plasma glucose (mmol/l)	5.7±0.1	5.7±0.2	10.0±0.6*†
Fasting serum insulin (pmol/l)	24±6	53±5*	95±10*†
Fasting serum C-peptide (nmol/l)	0.5±0.0	0.8±0.1*	1.2±0.1*†
Basal plasma glucose (mmol/l)	5.6±0.2	5.7±0.1	9.5±0.6*†
Clamp plasma glucose (mmol/l)	5.3±0.1	5.2±0.1	5.2±0.1
Basal serum insulin (pmol/l)	18±2	43±5*	77±7*†
Clamp serum insulin (pmol/l)	348±15	396±29	388±22
Basal GDR (mg m^{-2} min^{-1})	81±4	80±3	87±1
Clamp GDR (mg m^{-2} min^{-1})	352±18	244±21*	137±15*†

Data represent means±SEM

Plasma glucose, serum insulin, and C-peptide were measured as described [19]

*$p<0.05$ compared with LE by one-way ANOVA; †$p<0.05$ compared with OB by one-way ANOVA

T2D, obese and type 2 diabetes

Sample preparation and protein labelling Samples were homogenised in 2.4 μl (30 mmol/l Tris-base, 2 mol/l thiourea, 7 mol/l urea, 4% 3-[(3-cholamidopropyl)dimethylammonio]-1-propanesulfonate (CHAPS), pH 8.5) per mg tissue, sonicated for 2×1 min and centrifuged for 2×15 min (16,000*g*). After protein determination, supernatant fractions were labelled by adding 1 μl of 400 pmol/μl CyDye (Cy2, Cy3 or Cy5 'minimal dyes'; GE Healthcare, Munich, Germany, in dimethylformamide (DMF)) to 50 μg solubilised protein. Following 30 min at 4°C in the dark, reactions were stopped by 1 μl 10 mmol/l lysine. After 10 min ampholine 2-4 (GE Healthcare) and dithiothreitol (1.08 g/ml) were added (both at 1/10 volume of the total volume). Basal and clamp biopsy lysates from individual participants were alternately labelled with Cy3- or Cy5-dyes (colour swap to exclude labelling effects). A standard (mixture of equal protein amounts of all samples) was labelled with Cy2 dye and used to improve the matching of gels and normalisation of individual spotmaps.

2D-DIGE and image analysis This was performed as described [21]. Briefly, for every analysis, two samples with different dyes plus standard were combined (3×50 μg protein) and separated by carrier ampholyte-based isoelectric focusing, followed by 15.2/1.3% acrylamide/bisacrylamide gels [21]. Images were scanned (Typhoon TRIO-scanner, GE Healthcare, Freiburg, Germany), cropped with ImageQuant (GE Healthcare, Freiburg, Germany) and analysed (spot detection and inter- and intra-gel spot matching) with DeCyder-2D-V6.5 (GE Healthcare, Freiburg, Germany). The estimated spot number was set to 10,000, and spots <20,000 arbitrary units were removed.

Protein identification using nano-HPLC/ESI-MS/MS Two-dimensional gel electrophoresis was performed as described with 50 μg Cy2-labelled plus 200 μg unlabelled standard. Spots were manually picked and in-gel trypsin digested [22, 23]. Tryptic peptides were extracted twice with 10 μl acetonitrile/5% formamide (50/50 [vol./vol.]). Acetonitrile was removed in vacuo, 5% formamide added to yield 20 μl, and nano-HPLC-ESI-MS/MS performed [24]. MS/MS spectra peaklists were generated using DataAnalysis-4 (Bruker-Daltonics, Bremen, Germany). For identification, peaklists were

correlated with UniProtKB/Swiss-Prot composite database (release 10.08.2010) using MASCOT algorithm (V2.3.02) [25] and the ProteinScape (V1.3, Bruker-Daltonics, Bremen, Germany) database. Searches were restricted to human entries and performed with tryptic specificity allowing one missed cleavage and mass tolerances of 0.4 and 0.6 Da for MS and MS/MS experiments, respectively. Cysteine modification with propionamide was considered as fixed and oxidation of methionine as a variable modification.

Proteins were assembled based on identifications using ProteinExtractor (V1.0) in ProteinScape and sorted according to identification scores. Each protein was identified with at least two peptides (MASCOT peptide score >20), potential contaminants (keratins 1, 2, 9, 10, 14 and 16, and albumin) were excluded. For identification, a score >50 was required. If more than one protein fulfilled this requirement the protein with highest score was assigned; the others are listed in electronic supplementary material (ESM) Table 1. For detection of phosphorylation or ubiquitinylation, event searches were repeated with additional variable modification settings.

Western blots Solubilised protein (100 μg) was separated by 10% SDS-PAGE, transferred to polyvinylidene-fluoride membranes and probed with anti-glyceraldehyde-3-phosphate-dehydrogenase (GAPDH) or anti-α-actin antibody (Cell Signaling, Danvers, MA, USA and Abnova, Taipei, Taiwan, respectively). Detection was with IRDye 800CW goat-anti-rabbit-IgG (LI-COR Biosciences, Lincoln, NE, USA) and Odyssey imaging (LI-COR Biosciences).

Data analysis and spot selection Data analyses were with R (V2.10.1) [26]. Raw spot volumes were first standardised (ratio with the respective Cy2 spot on same gel) and log-transformed as proposed by DeCyder-2D-V6.5. Multiple comparisons were by one-way ANOVA and, if appropriate, subsequent Tukey's honest test. Paired data were compared with the paired *t* test. Correlations were analysed by Spearman's rank-order correlation. Fold differences were calculated based on the difference of their mean log-transformed volumes.

Spots that could be reliably measured/quantified in at least five basal and five clamp biopsies per group were selected if: (1) the difference between the highest and lowest mean log-transformed spot volume of the three study groups in basal or clamp biopsies was >0.41 (=1.5-fold difference of untransformed data) and p was <0.05; (2) basal and clamp biopsy spot volumes correlated with clamp GDR ($p<0.05$) or at least one other variable listed in ESM Table 2 ($p<0.02$); or (3) the difference between log-transformed volumes of basal and clamp biopsies was >0.41 (1.5-fold difference of untransformed data) in at least one study group, and $p<0.05$.

Results

Clinical and metabolic characteristics The OB and obese type 2 diabetes study groups were well matched with respect to BMI, and all study groups were well matched with respect to age (Table 1). Clamp GDR was lower in the OB than in the LE group and again lower in the obese type 2 diabetes group than in the OB group.

Muscle proteome and differences between LE, OB and type 2 diabetes Overall, 2,852 protein spots were detected by the software. In 107 of 128 spots that fulfilled the criteria for protein identification, the protein was successfully identified (for spectra results see PRIDE database, accession number 18608–18609)

Differential volumes between the three study groups were displayed by 44 protein spots (Table 2; ESM Table 3). Some proteins were identified in multiple spots, suggesting PTMs. This was found, for example, for glycogen phosphorylase, muscle form (PYGM), GAPDH, myosin regulatory light chain 2, ventricular/cardiac muscle (MYL2), β-enolase (ENO3) and myosin regulatory light chain 2, skeletal muscle (MYLPF) with four, eight, seven, three and four spots, respectively (Fig. 1; Table 2). Moreover, PYGM, MYL2 and MYLPF represent examples where different spots with the same protein displayed opposite changes in abundance between groups. Thus, in basal biopsies, the volume of PYGM in spot 453 was higher in the obese type 2 diabetes and OB groups compared with the LE group, whereas the volume of PYGM in spot 450 was highest in the LE group (Fig. 2), suggesting a shift in the abundance of PTMs. In addition, our data suggest that PYGM in spot 453 was phosphorylated at Ser15, and that the PTMs in MYL2 and MYLPF included serine phosphorylations and ubiquitinylations (Table 2).

As for PYGM spots 450 and 453 (Fig. 2), differences between groups tended to be smaller in clamp than basal biopsies, resulting in 21 compared with 33 significantly different spots between groups, respectively (Table 2). Apart from this observation, results in clamp and basal biopsies from the same individuals were fairly concordant and thus served as an internal control (Fig. 2; Table 2).

Differences in spot volumes were most pronounced between the obese type 2 diabetes and LE groups (significant in 29, 10 and five spots from basal, clamp or both basal and clamp biopsies, respectively; Table 2). Almost the same differences were observed between the OB and LE groups (significant in 23, 12 or six spots from basal, clamp, or both basal and clamp biopsies, respectively). Accordingly, only a few spots displayed substantial differences between the obese type 2 diabetes and OB groups.

Differentially expressed proteins comprised enzymes of glucose metabolism, mitochondrial proteins, sarcomeric proteins and proteins with other functions. With respect to

Table 2 Ratios of spot volumes between groups

Protein	Gene accession number	Spot	Basal biopsies			Clamp biopsies			*n*
			OB/LE	T2D/LE	T2D/OB	OB/ LE	T2D/ LE	T2D/OB	
Carbohydrate metabolism									
Glycolytic									
GAPDH	P04406	1389	1.13	1.37*	1.22	1.21	1.46*	1.21	31
		1398	1.25	1.23	0.99	1.25	1.28	1.02	24
		1435	1.26	1.28	1.02	1.34	1.31	0.98	29
		1443	1.35	1.32	0.98	1.42	1.30	0.92	28
		1450	1.52*	1.38*	0.91	1.43*	1.19	0.83	30
		1452	1.56*	1.46*	0.94	1.55*	1.36	0.88	30
		1458	1.53*	1.49*	0.97	1.48*	1.32	0.89	28
		1461[a]	1.75*	1.51	0.86	1.77*	1.42	0.80	19
PGAM2	P15259	1875	1.76*	1.95*	1.11	1.17	0.95	0.82	31
ENO3	P13929	1027	1.19	1.18	1.00	1.30	1.41*	1.09	27
		1032	1.17	1.12	0.96	1.20	1.16	0.97	31
		1072	2.20*	2.10*	0.95	2.24*	2.25*	1.00	30
PKM2	P14618	794	1.11	1.33	1.19	1.11	1.22	1.10	28
		795	1.19	1.23	1.03	1.18	1.11	0.95	31
		796	1.45	1.15	0.80	1.51	1.03	0.68	21
		820	1.14	1.22	1.07	1.19	1.12	0.95	30
		859	1.38	1.67*	1.21	1.09	1.29	1.19	19
Other									
MDH1	P40925	1627	0.98	0.77	0.79	0.85	0.78	0.91	26
		1630[b]	0.96	0.75	0.78	0.88	0.83	0.94	27
		1635	0.96	0.73*	0.77	0.90	0.77	0.86	30
PYGM	P11217	450	0.66	0.56*	0.84	0.80	0.74	0.93	30
		451[c]	1.02	1.18	1.15	0.89	0.99	1.11	20
		452	0.63	0,61	0.96	0.75	0.82	1.10	28
		453[c]	1.47*	1.57*	1.07	1.19	1.17	0.99	30
Mitochondrial									
ECH1	Q13011	1745	0.70	0.85	1.21	0.55*	0.83	1.49	22
GBAS	O75323	1929	0.80	0.78	0.98	0.78*	0.80	1.03	24
		1937	0.96	0.96	1.00	1.09	1.01	0.92	22
HADHB	P55084	957	1.02	1.13	1.10	0.57	1.17	2.04*	28
HES1	P30042	2026	0.93	0.74*	0.80	0.95	0.74*	0.78	31
Sarcomeric									
Fast									
MYL1	P05976	2126	0.81	0.63	0.77	0.77	1.02	1.32	28
		2582	1.56*	1.57*	1.01	1.57*	1.62*	1.04	20
		2601	1.36	1.73*	1.28	1.47	1.75*	1.19	30
MYLPF	Q96A32	2273	1.70*	2.22*	1.31	1.35	1.21	0.89	31
		2334	0.54*	0.50*	0.92	0.84	0.72	0.86	26
		2427	1.90*	1.94*	1.02	1.27	1.18	0.94	22
		2447[d]	1.58*	1.90*	1.20	1.19	1.18	1.00	31
TNNT3	P45378	1538	1.67*	1.51	0.91	1.34	1.18	0.88	30
		1540	1.48*	1.51*	1.02	1.29	1.13	0.88	31
		1550	1.46*	1.45*	0.99	1.29	1.14	0.88	31
		1602	1.16	1.12	0.96	1.10	1.07	0.98	28
		1606	1.35*	1.50*	1.12	1.02	1.12	1.09	31

Table 2 (continued)

Protein	Gene accession number	Spot	Basal biopsies			Clamp biopsies			*n*
			OB/LE	T2D/LE	T2D/OB	OB/ LE	T2D/ LE	T2D/OB	
Slow									
MYL2	P10916	2220	1.20	1.20	1.00	0.75	0.91	1.21	31
		2221[e]	0.37*	0.35*	0.94	0.53	0.75	1.43	23
		2223	0.66	0.57	0.86	0.52*	0.51*	0.97	20
		2227[e, f]	0.34*	0.30*	0.88	0.52	0.58	1.13	31
		2259	0.46*	0.31*	0.68	0.73	0.80	1.10	31
		2264[e]	1.85*	2.49*	1.34	1.37	1.51	1.10	31
		2269	0.51*	0.41*	0.80	0.89	0.79	0.89	30
MYL3	P08590	2141	0.76	0.58	0.76	0.68	0.80	1.17	30
		2445	0.55*	0.48*	0.87	0.94	0.77	0.81	31
TNNT1	P13805	1571	0.78	0.78	1.00	0.60*	0.90	1.49	31
Other									
DES	P17661	890	1.00	1.18	1.18	0.54*	1.11	2.07*	28
Miscellaneous functions									
ACTA2	P62736	200	1.12	0.96	0.85	1.09	0.88	0.81	16
		1182	0.94	0.80*	0.86	0.83	0.77*	0.92	27
		1835	0.45	0.36	0.80	0.92	0.85	0.93	19
ACTG2	P63267	1227	0.92	1.15	1.24*	0.85	1.11	1.30*	31
		1793	1.01	0.82	0.81	0.95	0.82	0.86	30
UPF0366 protein	Q9H7C9	2732	0.63	2.23	3.52*	0.77	1.88	2.43	18
CAP2	P40123	843	0.63*	0.73*	1.14	0.94	1.09	1.17	28
CFL2	Q9Y281	2290	0.70	0.86	1.23	0.62*	1.13	1.83*	22
CKM	P06732	1039	1.03	1.12	1.08	1.15	1.30	1.13	25
		1215	1.18	1.19	1.01	1.09	1.35*	1.23	29
		1216	1.06	1.06	1.00	1.03	1.15	1.11	29
FGG	P02679	904	1.00	0.99	0.99	0.62	1.05	1.70	30
		951	1.08	1.11	1.03	0.60	1.22	2.05*	26
HSPA2	P54652	638	1.19	1.39	1.17	1.18	1.56*	1.33	31
HBA1	P69905	2737[g]	1.39	6.28*	4.51*	1.25	2.65	2.13	21

Muscle samples were subjected to 2D-DIGE, spot volumes determined and spots chosen for subsequent identification as described. Shown are ratios of spot volumes between groups calculated based on the difference of mean log-transformed spot volumes. Listed are only spots with significant differences and spots with proteins where other spots with the same protein were significantly different.

Log-transformed volumes and additional data are shown in ESM Table 3

*$p<0.05$ in one way ANOVA and post hoc Tukey honest significance test between log-transformed spot volumes

Phosphorylation at: [a] Ser210 or Thr211; [b] Ser332 or Ser333; [c] Ser15; [d] Ser15, Ser16 or Ser17;

[e] Ubiquitinylation at Lys165

Phosphorylation at: [f] Ser15 or Ser19; and [g] Tyr43

n, number of participants for whom spot volumes could be assigned

ACTA2, actin, aortic smooth muscle; ACTG2, actin, γ-enteric smooth muscle; CAP2, adenylylcyclase-associated protein 2; CFL2, cofilin-2; CKM, creatine kinase M-type; DES, desmin; ECH1, Δ(3,5)-Δ(2,4)-dienoyl-CoA isomerase; HADHB, trifunctional enzyme subunit-β; MDH1, malate dehydrogenase; TNNT1, slow skeletal muscle troponin-T; FGG, fibrinogen γ chain; HSPA2, heat shock-related 70 kDa protein 2; HBA1, haemoglobin subunit α; T2D, obese and type 2 diabetes

glucose metabolism, mean volumes of 17 of 17, or 16 of 17 spots in basal or clamp biopsies, respectively, assigned to the glycolytic enzymes GAPDH, phosphoglycerate mutase-2 (PGAM2), ENO3 and pyruvate kinase (PKM2) were higher in the obese type 2 diabetes and OB groups than in the LE group, and differences between groups were significant in eight (basal biopsies) or seven of these spots (clamp biopsies). As GAPDH, ENO3 and PKM2 were identified in

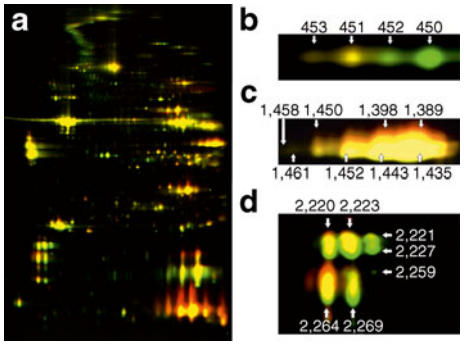

Fig. 1 **a** Representative two-dimensional gel. Similar amounts of protein from basal biopsies from an LE and an obese type 2 diabetic individual were labelled with different CyDyes, subjected to 2D-DIGE and scanned as described. Green, LE proteins dominate; red, type 2 diabetes proteins dominate; yellow, both signals similarly present. **b–d** Portions of this image were magnified to demonstrate multiple spots with PYGM (**b**), GAPDH (**c**) and MYL2 (**d**) identified in more detail

multiple spots, we analysed whether the sums of volumes of all identified spots with the respective enzyme (addition of raw spot volumes before analysis) were different. This revealed that, in addition to the single spot with PGAM2, these summative spot volumes were different between groups for GAPDH (LE −0.07±0.10, OB 0.17±0.08, obese type 2 diabetes 0.20±0.06, $p<0.05$, corresponding to ratios of OB/LE 1.27, obese type 2 diabetes/LE 1.31, and obese type 2 diabetes/OB 1.03) and ENO3 (LE −0.42±0.13, OB 0.00±0.08, obese type 2 diabetes 0.04±0.08, $p<0.05$, corresponding to ratios of OB/LE 1.52, obese type 2 diabetes/LE 1.47, and obese type 2 diabetes/OB 0.96), whereas for combined PKM2 spots differences were NS. GAPDH levels were also analysed in a western blot. Although, in contrast to the proteome data, differences were NS, a similar tendency was confirmed (Fig. 3).

In contrast to glycolytic enzyme spots, spots with Δ(3,5)-Δ(2,4)-dienoyl-CoA isomerase (ECH1) an enzyme involved in fatty acid oxidation, and two mitochondrial proteins, NipSnap-homologue-2 (GBAS), and ES1 protein homologue (HES1) tended to be less abundant in obese type 2 diabetes and OB (Table 2). Moreover, multiple spots containing the fast muscle proteins myosin light chain 1 (MYL1), MYLPF, or fast skeletal muscle troponin-T (TNNT3) were upregulated, whereas spots containing the slow-muscle proteins MYL2, myosin light chain 3 (MYL3), or slow skeletal muscle troponin-T (TNNT1) were downregulated in OB and/or obese type 2 diabetes groups compared with the LE group. If summative volumes of all spots containing the respective enzymes were analysed as described above, these were higher in the OB and obese type 2 diabetes groups than the LE group for MYLPF ($p<0.05$, ratios OB/LE 1.50, obese type 2 diabetes/LE 1.85, obese type 2 diabetes/OB 1.23), and TNNT3 ($p<0.05$, ratios OB/LE 1.41, obese type 2 diabetes/LE 1.46, obese type 2 diabetes/OB 1.04) and lower in the OB and obese type 2 diabetes groups than the LE group for MYL3 (ratios OB/LE 0.67, obese type 2 diabetes/LE 0.52, obese type 2 diabetes/OB 0.78). Differences of summative spots containing MYL1 or MYL2 were NS.

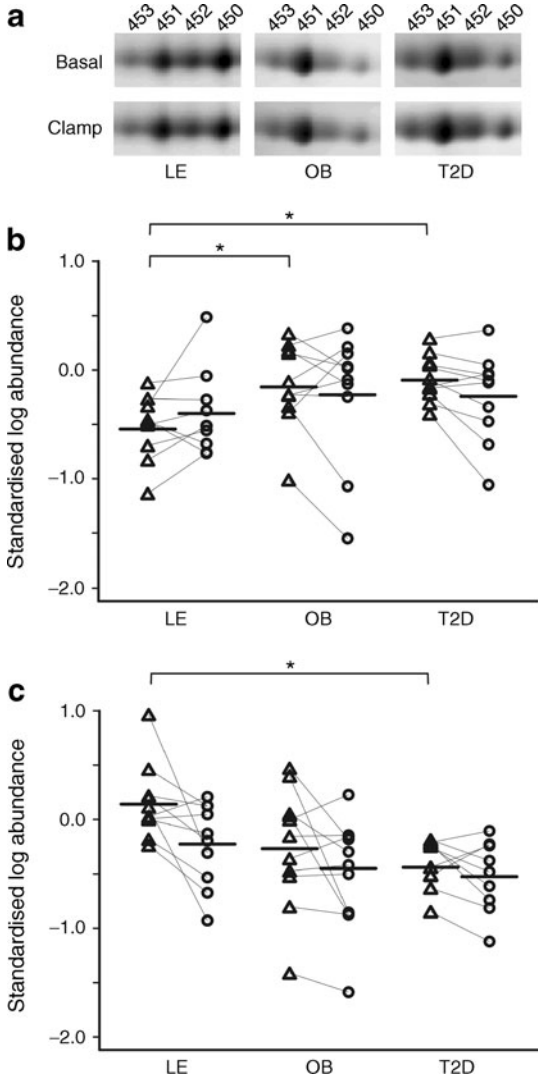

Fig. 2 Volumes of spots identified as PYGM in LE, OB and obese type 2 diabetic participants. Muscle samples were analysed and protein names assigned as described in Table 2. Shown are representative portions of the 2D-DIGE gels with the spots containing PYGM (**a**) and individual volumes of spot 453 (**b**) and 450 (**c**) in basal and clamp biopsies. Thin lines connect data of basal and clamp biopsies of the same individual; means are shown as strong horizontal lines; *$p<0.05$ compared with LE. Triangles, basal; circles, clamp biopsies. T2D, obese and type 2 diabetes

Correlations of spot volumes with physiological and clinical variables Although mean clamp GDRs were significantly different between study groups, individual values overlapped (Fig. 4). To identify additional proteins that might be more strongly related to GDR or other variables than to the

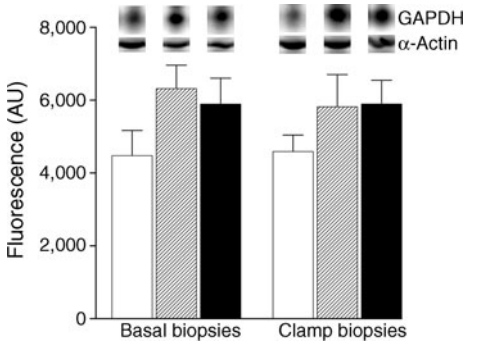

Fig. 3 Western blot analysis of GAPDH protein expression. Similar protein amounts (100 μg) of solubilised basal and clamp muscle were subjected to western blot analysis with GAPDH-specific antibody as described. α-Actin served as loading control and was not different between groups. Shown are representative immunoblots and means ±SEM of the LE, OB and obese type 2 diabetes groups. White bars, LE (n=10); hatched bars, OB (n=11); black bars, obese type 2 diabetes (n=10). AU, arbitrary units

multifactorial type 2 diabetes or obesity state, we analysed correlations of spot volume data of all study participants with GDR and other variables. For example, volumes of spot 1458 (GAPDH) correlated negatively with clamp GDR and glucose oxidation, but positively with clamp lipid oxidation (Fig. 4). Similar negative correlations with clamp GDR, NOGM and glucose oxidation, but positive correlations with lipid oxidation, were found in basal biopsies for almost all spots with identified glycolytic or fast-muscle proteins, whereas opposite correlations existed for most spots with tricarboxylic acid (TCA) or respiratory chain enzymes, or slow-muscle proteins (Fig. 5; ESM Table 2). Data were similar in clamp biopsies, except that fewer correlations were statistically significant (ESM Table 2). The same correlation pattern as with single spot volumes was also observed for summative volumes of multiple spots with the same identified protein. Thus, for the glycolytic enzymes GAPDH and ENO3, and the fast-muscle proteins MYLPF and TNNT3, these summative volumes in basal biopsies correlated negatively (p<0.05) with clamp GDR. In most cases, they also correlated negatively with clamp NOGM and glucose oxidation, and positively with clamp lipid oxidation. Correlations were opposite for mitochondrial proteins aconitate hydratase (ACO2), ATP subunit-α (ATP5A1), ATPase subunit-β (ATP5B) and GBAS, and the slow-muscle protein MYL3 (ESM Table 4).

Effect of insulin stimulation Several spots displayed different volumes between basal and clamp biopsies (Table 3). These proteins included the sarcomeric proteins actin, α skeletal muscle (ACTA1), tropomyosin α-1 chain (TPM1), MYL1, MYL3 and myosin heavy chain 2 (MYH2), and the mitochondrial proteins ATP5A1 and trifunctional enzyme subunit-β (HADHB).

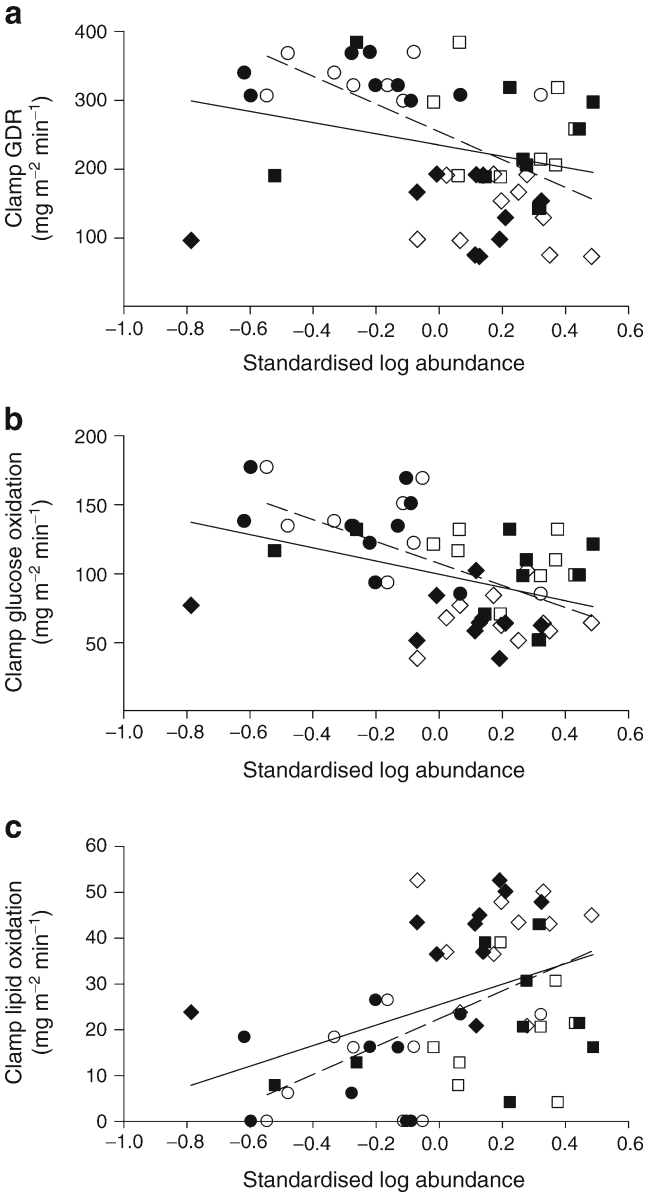

Fig. 4 Correlations between spot 1458 (GAPDH) abundance and clamp GDR (**a**), clamp glucose oxidation (**b**) and clamp lipid oxidation (**c**). Shown are spot volumes of basal and clamp biopsies of the LE, OB and type 2 diabetes groups. Dashed and solid lines represent linear regressions for basal and clamp biopsies, respectively; all correlations were p<0.05. White symbols, basal; black symbols, clamp; circles, LE; squares, OB; diamonds, obese type 2 diabetes

Discussion

Skeletal muscle insulin resistance is critical to the pathogenesis of type 2 diabetes and obesity. Here, we investigated with the sensitive 2D-DIGE proteomic approach whether changes in abundance of proteins or patterns of proteins in biological pathways could contribute to these forms of insulin resistance.

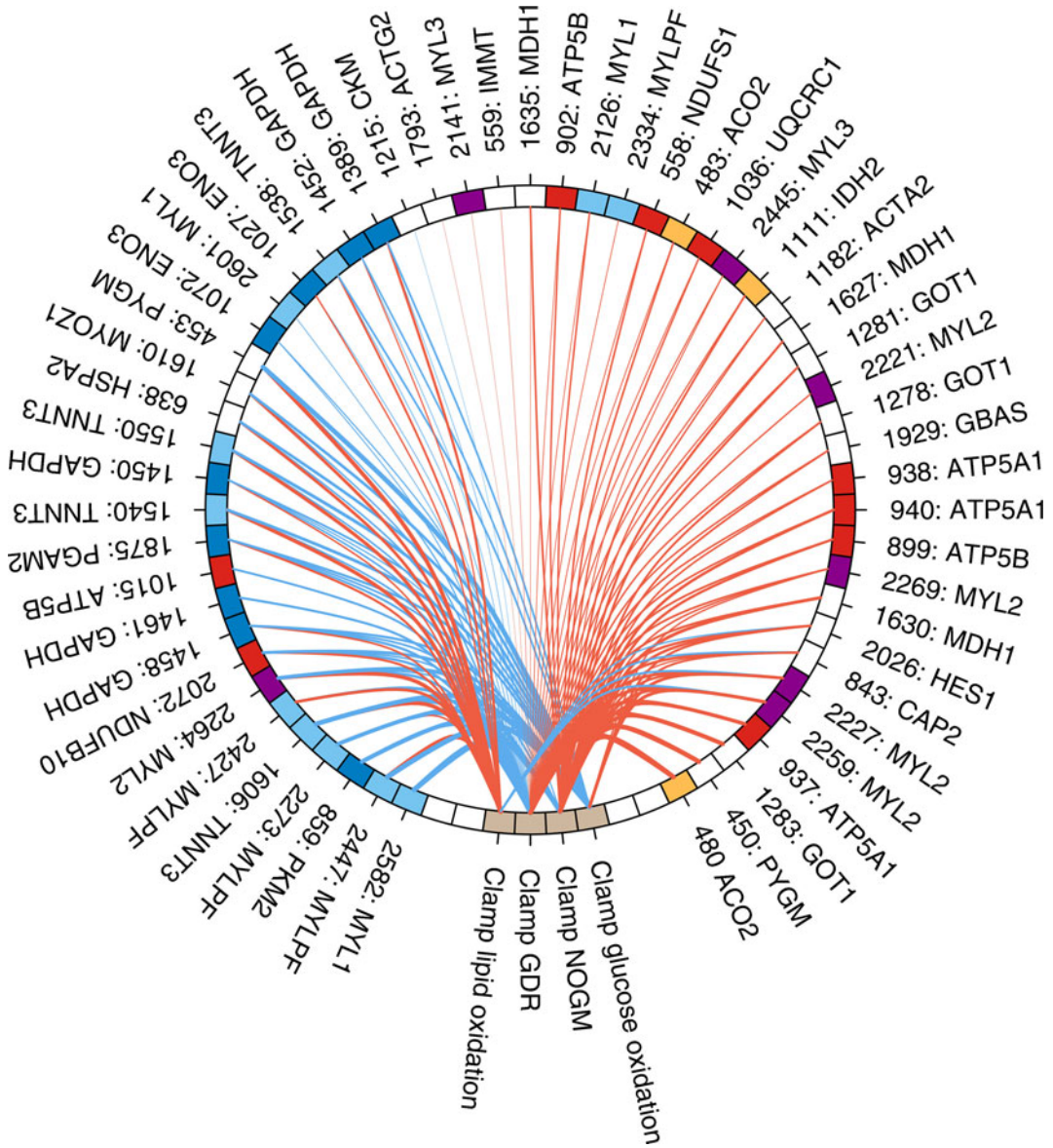

Fig. 5 Correlation of spot volumes with GDR, glucose oxidation, non-oxidative glucose metabolism and lipid oxidation. Coloured circle segments with spot numbers and protein abbreviations represent spots with volumes that correlated with GDR ($p<0.05$) in basal biopsies, starting with strongest negative correlation on the left and moving to the strongest positive on the right. Lines connect these segments with segments that represent the four variables, and line strength indicates the strength of negative (blue) or positive (red) correlation. Colours of circle segments indicate protein categories: dark blue, glycolytic; light blue, fast muscle; dark red, respiratory chain; orange, TCA cycle; purple, slow muscle; white, other functions. Detailed and additional correlation data are provided in ESM Table 2. ACTG2, γ-enteric smooth muscle actin; CAP2, adenylyl cyclase-associated protein 2; CKM, creatine kinase M-type; GOT1, aspartate aminotransferase; HES1, ES1 protein homologue, mitochondrial; HSPA2, heat shock-related 70 kDa protein 2; IDH2, isocitrate dehydrogenase; IMMT, mitochondrial inner membrane protein; MDH1, malate dehydrogenase; MYOZ1, myozenin-1; NDUFB10, NADH dehydrogenase [ubiquinone] 1 β subcomplex subunit 10; NDUFS1, NADH-ubiquinone oxidoreductase 75 kDa subunit; UQCRC1, cytochrome b-c 1 complex subunit 1

A major observation of our analysis is that spot volumes related to multiple glycolytic proteins were higher in OB and obese type 2 diabetes groups than in the LE group, and/or correlated negatively with clamp GDR (Figs 5 and 6). This suggests that upregulation of glycolysis by increased enzyme abundance could be a major characteristic of insulin resistance. In particular, spots containing GAPDH, PGAM2 and ENO3 were increased in obese and/or diabetic individuals. All five spots containing PKM2 also tended to be higher in obese type 2 diabetes and OB, but although the difference was significant in one spot, the difference in overall abundance did not reach statistical significance.

Table 3 Ratios of spot volumes between clamp and basal biopsies

Protein	Spot	Ratio clamp/basal		
		LE	OB	T2D
Carbohydrate metabolism				
PYGM	450	0.69*	0.83	0.92
Mitochondrial				
ATP5A1	763	0.43	0.78	0.45*
HADHB	957	0.90	0.50*	0.93
PARK7	2094	1.04	1.23	2.62*
Sarcomeric				
Fast				
MYL1	2126	1.09	1.04	1.78*
Slow				
MYH2	765	0.58*	0.72	0.39
MYL3	2141	1.39	1.24	1.92*
	2445	0.57*	0.98	0.92
Other				
ACTA1	1081	1.16	1.38*	1.97*
	1185	1.11	1.23	1.84*
TPM1	1632	1.22	1.18	1.76*
Miscellaneous functions				
ACTG2	1793	1.16	1.08	1.16*
CA3	1839	1.07	1.23	1.43*
CCT5	764	0.59*	0.76	0.48
FGB	804	0.77	0.66*	0.91
FGG	904	0.87	0.53*	0.92
HSPA8	627	1.04	1.01	1.13*

Muscle samples were analysed and protein names assigned as described in Table 2

Shown are ratios of spot volumes between clamp and basal biopsies of each group calculated based on the difference of mean log-transformed spot volumes (ESM Table 3)

*$p<0.05$ in paired t test between log-transformed spot volumes of basal and clamp biopsies

ACTG2, actin, γ-enteric smooth muscle; CA3, carbonic anhydrase 3; CCT5, T-complex protein 1 subunit ε; FGB, fibrinogen β chain; FGG, fibrinogen γ chain; HADHB, trifunctional enzyme subunit-β; HSPA8, heat shock cognate 71 kDa protein; PARK7, protein DJ-1; TPM1, tropomyosin α-1 chain; T2D, obese and type 2 diabetes

Most spots containing glycolytic enzymes correlated also significantly negatively with clamp GDR and glucose oxidation, and positively with clamp lipid oxidation.

In contrast to glycolytic proteins, proteins involved in the TCA cycle, mitochondrial respiration and other mitochondrial functions appeared less abundant in insulin resistance. In basal biopsies, 14 of 21 spots identified as proteins involved in these processes correlated positively ($p<0.05$) with clamp GDR and/or NOGM. Moreover, significant positive correlations were also observed for summative spot volumes (sum of volumes of all spots with the same identified protein) relating to cytoplasmic malate dehydrogenase (MDH1), an enzyme controlling TCA cycle pool size and providing contractile function [27], and the mitochondrial enzymes ACO2, ATP5A1, ATP5B and GBAS. These results, suggesting reduced TCA cycle and mitochondrial protein content in insulin resistance, are consistent with previous findings of reduced enzyme activities [10, 28, 29], protein expression [16, 17, 30], altered phosphorylation [16, 31, 32], altered transcript levels [10, 33, 34] or altered flux through mitochondrial ATP synthase [8].

Taken together, our observations of increased glycolytic and decreased TCA cycle or mitochondrial protein content in insulin resistance (Figs 5 and 6) support the hypothesis that altered glycolytic and oxidative capacities contribute to its phenotype. Although the mitochondrial content and dysfunction in insulin-resistant states has been studied extensively [2–12, 32, 35, 36], few data exist about the potential role of glycolytic enzymes in insulin resistance. Consistent with increased glycolytic enzyme activity in insulin resistance are previous findings that the ratio between glycolytic (phosphofructokinase, GAPDH, hexokinase, PYGM) and oxidative enzyme activities (citrate synthase, cytochrome oxidase) was negatively correlated with insulin sensitivity [11], and that phosphofructokinase activity decreased upon 10% weight loss in obese individuals [37]. In contracting muscle, factors related to the energy state appear to control glycolysis [38], and therefore impaired mitochondrial function with less energy production could be responsible for increased glycolysis and, potentially, glycolytic enzyme abundance. Conversely, increased glycolytic enzyme levels and activity under basal conditions could result in substrate overload for the mitochondria, contribute to ‘metabolic inflexibility’ in insulin resistance, i.e. a reduced ability of skeletal muscle to switch from fatty acid oxidation in the fasting state to glucose oxidation in the insulin-stimulated state and back [39], and may dispose skeletal muscle towards lipid accumulation [7, 39].

In our analysis, several proteins were identified in multiple spots. For example, the key glycogenolytic enzyme PYGM was found in four spots, one of which was increased in OB and obese type 2 diabetes (spot 453), while another was reduced in obese type 2 diabetes (spot 450). Moreover, at least in LE individuals, spot 453 and 450 tended to be increased and decreased, respectively, by the clamp. These data suggest a shift in abundance between two differently post-translationally modified PYGM proteins that may have different properties. Interestingly, spot 453 contained PYGM phosphorylated at Ser15, which results in activation [40]. Although glycogen synthase has extensively been studied in insulin-resistant skeletal muscle in the past years, less information is available about PYGM. The notion that the observed shift between spot 450 and 453 might be associated with higher activity of the enzyme in insulin

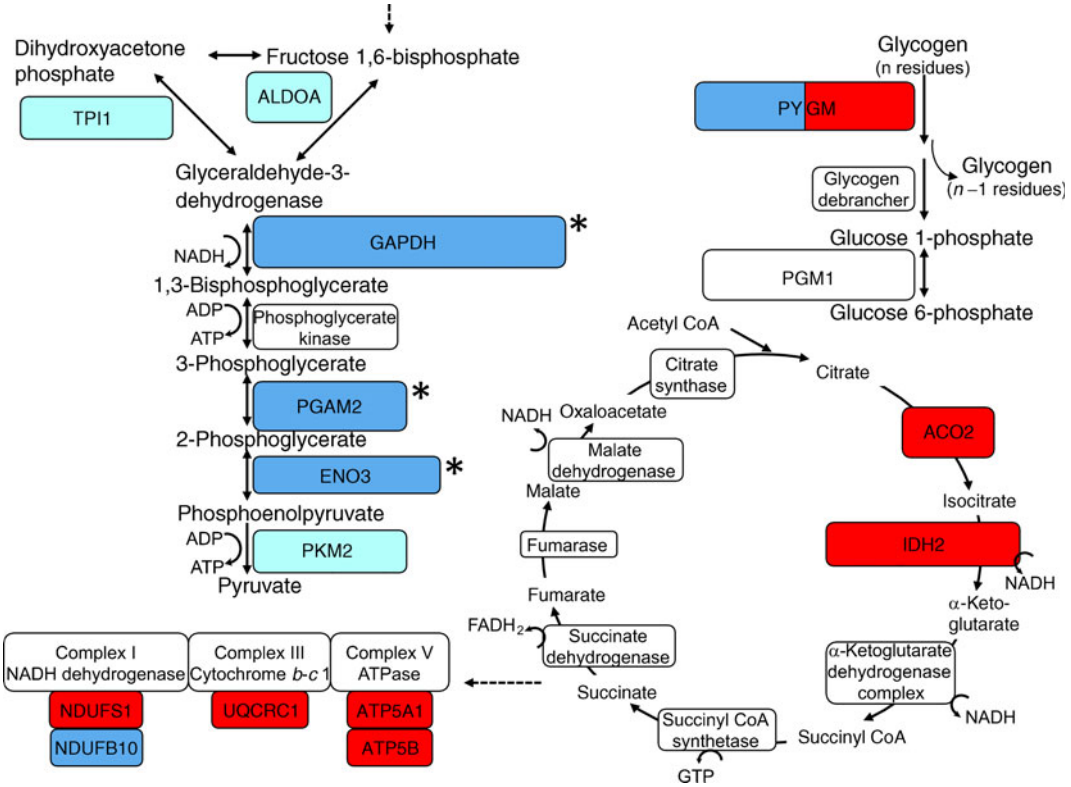

Fig. 6 Role of identified proteins in metabolic pathways. Data refer to basal biopsies; for detailed data see Table 2 and ESM Tables 2 and 4. A complete dark red or dark blue label indicates proteins where combined spot volumes (combination of all spots where the respective protein was identified) were significantly negatively (red) or positively (blue) correlated with GDR ($p<0.05$). Partial dark red and dark blue labelling of a single protein indicates that at least one spot was significantly negatively and one spot significantly positively correlated with GDR (correlation of combined spot volumes NS). Light blue indicates proteins where all identified spots had negative correlation coefficients (correlation of combined spot volumes NS). *$p<0.05$ between groups of LE, OB and obese participants with type 2 diabetes. ALDOA, aldolase; IDH2, isocitrate dehydrogenase; NDUFB10, NADH dehydrogenase [ubiquinone] 1 β subcomplex subunit 10; NDUFS1, NADH-ubiquinone oxidoreductase 75 kDa subunit; PGM1, phosphoglucomutase-1; TPT1, triosephosphate isomerase; UQCRC1, cytochrome *b-c* 1 complex subunit 1

resistance is, however, not supported by previous studies. Thus, activity of PYGM was not found to be different in muscle from obese individuals with type 2 diabetes [11, 41] or regulated by changes in glucose or insulin levels [42]. On the other hand, lack of PYGM activity is associated with insulin resistance [43]. In any case, regulation of PYGM by PTMs might be quite complex. For example, three other phosphorylation sites of PYGM have recently been detected [31]. Activating and deactivating modifications may therefore counterbalance and thus ensure a normal glycogenolysis in insulin-resistant muscle under basal conditions. This balance may be disturbed, for example, in hypoglycaemia, where PYGM activity increased by 50% only in those with type 2 diabetes and not in control participants [41].

GAPDH was found in eight spots in our study, suggesting PTMs, and in fact one spot (1461) was detected as being phosphorylated. Multiple PTMs of GAPDH have also been described in a recent analysis in GAPDH-overexpressing human embryonic kidney cells, including deamidation, methylation, methionine oxidation and phosphorylation [44]. In our study, all eight GAPDH spots had higher mean volumes in obese participants with type 2 diabetes and OB individuals compared with LE participants, and this was significant in five spots. Consistently, western blots revealed a tendency of increased GAPDH protein abundance in these states. As no substantial differences between the different GAPDH spots were found regarding their volume ratios between groups or following insulin stimulation, it is not possible to conclude from our data that the underlying PTMs are relevant for causing insulin resistance or are modified by insulin.

As skeletal muscle contains type I (slow oxidative), IIa (fast oxidative glycolytic) and IIx (fast glycolytic) fibres [3, 35, 36], altered fibre type distribution could have contributed to our results. Type I, IIa, and IIx fibres contain MYH7, MYH2 and MYH1, respectively [45]. In our study, no spots containing MYH7, MYH2 and MYH1 were identified as different between groups or correlated to variables of insulin resistance, and MYH2 was only identified because of a difference between clamp and basal biopsies. This argues

against a major role of differences in fibre-type distribution. In contrast to heavy chains, marked differences between groups were observed for other sarcomeric proteins. Most spots of fast myosin light chain isoform MYLPF and all spots of the fast-muscle protein TNNT3 were upregulated in OB and/or obese type 2 diabetes groups, and upregulation was also confirmed if all identified spots containing one of these proteins were combined before analysis. Conversely, combined spots of the slow myosin light chain isoform MYL3 were downregulated. Combined spots were not different between groups for MYL1 or MYL2, but the marked differences in individual spots suggest a role of differential PTMs. Taken together, our data thus support the notion that in OB and obese type 2 diabetic individuals muscle properties are shifted to a fast-twitch glycolytic pattern in the absence of marked changes in fibre-type distribution. The absence of marked changes in fibre-type distribution in OB and obese type 2 diabetic participants is also supported by several [3, 35], but not all [36], previous studies.

The fact that only a few spots displayed differences following insulin stimulation may be explained by the relatively short time for changes in protein expression or PTMs. Spot volumes related to PYGM and ATP5A1 tended to be lower in the clamp biopsies. Stronger changes were found in sarcomeric proteins, including insulin-stimulated upregulation of ACTA1, MYL1 and MYL3, and downregulation of MYH2 spots. These changes may largely be due to phosphorylations [31, 46] and/or other PTMs. Insulin elicits rapid dynamic remodelling of actin filaments, and this is necessary for GLUT4 translocation [47, 48]. MYH2 phosphorylation has been implicated to participate in GLUT4 storage vesicle translocation [49]. Taken together, these data support the notion that insulin actions include alterations of proteins involved in contraction and/or intracellular transport.

More differences in spot volumes were found between the OB and LE groups than between the obese type 2 diabetes and OB groups. This suggests that while obesity and the obesity-related insulin resistance is associated with altered expression of more abundant proteins and/or their PTMs, the additional reduction in clamp GDR in obese type 2 diabetes was mainly associated with changes of less abundant proteins, e.g. signalling intermediates that were not detectable by the proteomic approach.

The fluorescence labelling method used here has recently been applied to analyse the mitochondrial skeletal muscle proteome after endurance exercise training [14], but has so far not been applied to compare the muscle proteome of LE with OB or obese type 2 diabetic individuals. It has a higher sensitivity and a more dynamic range compared with the methods used in previous studies [15, 16]. Nevertheless, of the 36 spots relating to 20 proteins found significantly different by >1.5-fold between the groups in our study, several have also been identified in these previous two-dimensional-gel-based studies. This includes six from 13 proteins identified as different in a study with lean, obese and morbidly obese participants [15], and four from eight proteins identified as different in our own previous investigation with type 2 diabetic and control individuals [16]. Thus, these two-dimensional-gel proteomic studies delivered largely consistent findings. Another recent study used one-dimensional SDS-PAGE and label-free MS/MS-based identification and quantification [17]. Of 92 proteins increased more than twofold and of these, the 15 significantly different between OB and/or obese type 2 diabetic and LE participants in that study, only six and one, respectively, were also identified by us. This is potentially explained by the different method, in which quantification is based on peptide abundance rather than whole-protein abundance, and PTMs are not detected.

In summary, we have shown in human skeletal muscle that insulin resistance in obesity is associated with different expression and/or PTMs of multiple proteins and that the increased abundance of glycolytic enzymes and the decreased abundance of mitochondrial proteins appear to be part of its phenotype. In addition, our data suggest that this is accompanied by a shift in abundance from slow to fast myosin light chain isoforms in the absence of detected changes in myosin heavy chain isoforms, consistent with a shift of muscle properties towards a fast-twitch glycolytic pattern without marked changes in fibre-type distribution. Fewer differences were found between obese diabetic and OB than between LE and obese individuals, suggesting that the additional type-2-diabetes-associated insulin resistance is largely related to other mechanisms such as signalling events not detected by the method. Compared with focused biochemical data, the changes in protein abundance and PTMs observed in multiple pathways add information on how these interact in insulin resistance. The roles of several of the differentially regulated proteins remain to be elucidated.

Acknowledgements We acknowledge L. Hansen, C. B. Olsen, K. Pfeiffer, S. Link and C. Fischer-Lahdo for skilled technical assistance.

Funding The study was supported by grants from the Forum programme at Bochum University, the German Diabetes Association, the Danish Medical Research Council, and the Excellence Grant 2009 from the Novo Nordisk Foundation.

Contribution statement KH, WS, KL, HB-N, KS, HEM and HHK conceived and designed the study. JG, GP, KH, KL, KS and WS performed the experiments. JG, GP, KH, JWD, KL, KP and HHK analysed and interpreted the data. JG, GP, KH and HHK drafted the manuscript and all authors revised the manuscript for intellectual content and approved the final version.

Duality of interest All authors declare that there is no duality of interest associated with this manuscript.

References

1. Abdul-Ghani MA, DeFronzo RA (2010) Pathogenesis of insulin resistance in skeletal muscle. J Biomed Biotechnol 2010:476279
2. Cheng Z, Tseng Y, White MF (2010) Insulin signaling meets mitochondria in metabolism. Trends Endocrinol Metab 21:589–598
3. Chomentowski P, Coen PM, Radikova Z, Goodpaster BH, Toledo FG (2011) Skeletal muscle mitochondria in insulin resistance: differences in intermyofibrillar versus subsarcolemmal subpopulations and relationship to metabolic flexibility. J Clin Endocrinol Metab 96:494–503
4. Mogensen M, Sahlin K, Fernstrom M et al (2007) Mitochondrial respiration is decreased in skeletal muscle of patients with type 2 diabetes. Diabetes 56:1592–1599
5. Ritov VB, Menshikova EV, He J, Ferrell RE, Goodpaster BH, Kelley DE (2005) Deficiency of subsarcolemmal mitochondria in obesity and type 2 diabetes. Diabetes 54(1):8–14
6. Befroy DE, Petersen KF, Dufour S et al (2007) Impaired mitochondrial substrate oxidation in muscle of insulin-resistant offspring of type 2 diabetic patients. Diabetes 56:1376–1381
7. Kelley DE, He J, Menshikova EV, Ritov VB (2002) Dysfunction of mitochondria in human skeletal muscle in type 2 diabetes. Diabetes 51:2944–2950
8. Petersen KF, Dufour S, Shulman GI (2005) Decreased insulin-stimulated ATP synthesis and phosphate transport in muscle of insulin-resistant offspring of type 2 diabetic parents. PLoS Med 2:e233
9. Phielix E, Schrauwen-Hinderling VB, Mensink M et al (2008) Lower intrinsic ADP-stimulated mitochondrial respiration underlies in vivo mitochondrial dysfunction in muscle of male type 2 diabetic patients. Diabetes 57:2943–2949
10. Ritov VB, Menshikova EV, Azuma K et al (2010) Deficiency of electron transport chain in human skeletal muscle mitochondria in type 2 diabetes mellitus and obesity. Am J Physiol Endocrinol Metab 298:E49–E58
11. Simoneau JA, Kelley DE (1997) Altered glycolytic and oxidative capacities of skeletal muscle contribute to insulin resistance in NIDDM. J Appl Physiol 83:166–171
12. Szendroedi J, Schmid AI, Meyerspeer M et al (2009) Impaired mitochondrial function and insulin resistance of skeletal muscle in mitochondrial diabetes. Diabetes Care 32:677–679
13. Højlund K, Yi Z, Hwang H et al (2008) Characterization of the human skeletal muscle proteome by one-dimensional gel electrophoresis and HPLC-ESI-MS/MS. Mol Cell Proteomics 7:257–267
14. Egan B, Dowling P, O'Connor PL et al (2011) 2-D DIGE analysis of the mitochondrial proteome from human skeletal muscle reveals time course-dependent remodelling in response to 14 consecutive days of endurance exercise training. Proteomics 11:1413–1428
15. Hittel DS, Hathout Y, Hoffman EP, Houmard JA (2005) Proteome analysis of skeletal muscle from obese and morbidly obese women. Diabetes 54:1283–1288
16. Højlund K, Wrzesinski K, Larsen PM et al (2003) Proteome analysis reveals phosphorylation of ATP synthase beta -subunit in human skeletal muscle and proteins with potential roles in type 2 diabetes. J Biol Chem 278:10436–10442
17. Hwang H, Bowen BP, Lefort N et al (2010) Proteomics analysis of human skeletal muscle reveals novel abnormalities in obesity and type 2 diabetes. Diabetes 59:33–42
18. Thingholm TE, Bak S, Beck-Nielsen H, Jensen ON, Gaster M (2011) Characterization of human myotubes from type 2 diabetic and non-diabetic subjects using complementary quantitative mass spectrometric methods. Mol Cell Proteomics 10(9):M110.006650
19. Højlund K, Frystyk J, Levin K, Flyvbjerg A, Wojtaszewski JF, Beck-Nielsen H (2006) Reduced plasma adiponectin concentrations may contribute to impaired insulin activation of glycogen synthase in skeletal muscle of patients with type 2 diabetes. Diabetologia 49:1283–1291
20. Hother-Nielsen O, Henriksen JE, Holst JJ, Beck-Nielsen H (1996) Effects of insulin on glucose turnover rates in vivo: isotope dilution versus constant specific activity technique. Metabolism 45:82–91
21. Klose J, Kobalz U (1995) Two-dimensional electrophoresis of proteins: an updated protocol and implications for a functional analysis of the genome. Electrophoresis 16:1034–1059
22. Schaefer H, Chervet JP, Bunse C, Joppich C, Meyer HE, Marcus K (2004) A peptide preconcentration approach for nano-high-performance liquid chromatography to diminish memory effects. Proteomics 4:2541–2544
23. Schaefer H, Chamrad DC, Marcus K, Reidegeld KA, Bluggel M, Meyer HE (2005) Tryptic transpeptidation products observed in proteome analysis by liquid chromatography-tandem mass spectrometry. Proteomics 5:846–852
24. Poschmann G, Sitek B, Sipos B et al (2009) Identification of proteomic differences between squamous cell carcinoma of the lung and bronchial epithelium. Mol Cell Proteomics 8:1105–1116
25. Perkins DN, Pappin DJ, Creasy DM, Cottrell JS (1999) Probability-based protein identification by searching sequence databases using mass spectrometry data. Electrophoresis 20:3551–3567
26. R Development Core Team (2010) R: A language and environment for statistical computing. R Foundation for Statistical Computing, Vienna
27. Danis P, Farkas R (2009) Hormone-dependent and hormone-independent control of metabolic and developmental functions of malate dehydrogenase—review. Endocr Regul 43:39–52
28. Gaster M (2009) Reduced TCA flux in diabetic myotubes: a governing influence on the diabetic phenotype? Biochem Biophys Res Commun 387:651–655
29. Schrauwen P, Hesselink MK (2008) Reduced tricarboxylic acid cycle flux in type 2 diabetes mellitus? Diabetologia 51:1694–1697
30. Mullen E, Ohlendieck K (2010) Proteomic profiling of non-obese type 2 diabetic skeletal muscle. Int J Mol Med 25:445–458
31. Højlund K, Bowen BP, Hwang H et al (2009) In vivo phosphoproteome of human skeletal muscle revealed by phosphopeptide enrichment and HPLC-ESI-MS/MS. J Proteome Res 8:4954–4965
32. Højlund K, Yi Z, Lefort N et al (2010) Human ATP synthase beta is phosphorylated at multiple sites and shows abnormal phosphorylation at specific sites in insulin-resistant muscle. Diabetologia 53:541–551
33. Patti ME, Butte AJ, Crunkhorn S et al (2003) Coordinated reduction of genes of oxidative metabolism in humans with insulin resistance and diabetes: Potential role of PGC1 and NRF1. Proc Natl Acad Sci USA 100:8466–8471
34. Zelezniak A, Pers TH, Soares S, Patti ME, Patil KR (2010) Metabolic network topology reveals transcriptional regulatory signatures of type 2 diabetes. PLoS Comput Biol 6:e1000729
35. He J, Watkins S, Kelley DE (2001) Skeletal muscle lipid content and oxidative enzyme activity in relation to muscle fiber type in type 2 diabetes and obesity. Diabetes 50:817–823
36. Oberbach A, Bossenz Y, Lehmann S et al (2006) Altered fiber distribution and fiber-specific glycolytic and oxidative enzyme activity in skeletal muscle of patients with type 2 diabetes. Diabetes Care 29:895–900
37. Goldsmith R, Joanisse DR, Gallagher D et al (2010) Effects of experimental weight perturbation on skeletal muscle work efficiency, fuel utilization, and biochemistry in human subjects. Am J Physiol Regul Integr Comp Physiol 298:R79–R88
38. Ortenblad N, Macdonald WA, Sahlin K (2009) Glycolysis in contracting rat skeletal muscle is controlled by factors related to energy state. Biochem J 420:161–168
39. Kelley DE, Mandarino LJ (2000) Fuel selection in human skeletal muscle in insulin resistance: a reexamination. Diabetes 49:677–683

40. Johnson LN (2009) The regulation of protein phosphorylation. Biochem Soc Trans 37:627–641
41. Shamoon H, Friedman S, Canton C, Zacharowicz L, Hu M, Rossetti L (1994) Increased epinephrine and skeletal muscle responses to hypoglycemia in non-insulin-dependent diabetes mellitus. J Clin Invest 93:2562–2571
42. Yki-Jarvinen H, Mott D, Young AA, Stone K, Bogardus C (1987) Regulation of glycogen synthase and phosphorylase activities by glucose and insulin in human skeletal muscle. J Clin Invest 80:95–100
43. Nielsen JN, Vissing J, Wojtaszewski JF, Haller RG, Begum N, Richter EA (2002) Decreased insulin action in skeletal muscle from patients with McArdle's disease. Am J Physiol Endocrinol Metab 282:E1267–E1275
44. Seo J, Jeong J, Kim YM, Hwang N, Paek E, Lee KJ (2008) Strategy for comprehensive identification of post-translational modifications in cellular proteins, including low abundant modifications: application to glyceraldehyde-3-phosphate dehydrogenase. J Proteome Res 7:587–602
45. Ennion S, Sant'ana Pereira J, Sargeant AJ, Young A, Goldspink G (1995) Characterization of human skeletal muscle fibres according to the myosin heavy chains they express. J Muscle Res Cell Motil 16:35–43
46. Choi YO, Ryu HJ, Kim HR et al (2006) Implication of phosphorylation of the myosin II regulatory light chain in insulin-stimulated GLUT4 translocation in 3T3-F442A adipocytes. Exp Mol Med 38:180–189
47. Patel N, Rudich A, Khayat ZA, Garg R, Klip A (2003) Intracellular segregation of phosphatidylinositol-3,4,5-trisphosphate by insulin-dependent actin remodeling in L6 skeletal muscle cells. Mol Cell Biol 23:4611–4626
48. Kanzaki M (2006) Insulin receptor signals regulating GLUT4 translocation and actin dynamics. Endocr J 53:267–293
49. Chung le TK, Hosaka T, Harada N et al (2010) Myosin IIA participates in docking of Glut4 storage vesicles with the plasma membrane in 3T3-L1 adipocytes. Biochem Biophys Res Commun 391:995–999